

# Collider Searches for Extra Dimensions

G. Landsberg<sup>\*†</sup>

*Brown University, Department of Physics, 182 Hope St., Providence, RI 02912, USA*

Searches for extra spatial dimensions remain among the most popular new directions in our quest for physics beyond the Standard Model. High-energy collider experiments of the current decade should be able to find an ultimate answer to the question of their existence in a variety of models. Until the start of the LHC in a few years, the Tevatron will remain the key player in this quest. In this paper, we review the most recent results from the Tevatron on searches for large,  $\text{TeV}^{-1}$ -size, and Randall-Sundrum extra spatial dimensions, which have reached a new level of sensitivity and currently probe the parameter space beyond the existing constraints. While no evidence for the existence of extra dimensions has been found so far, an exciting discovery might be just steps away.

## 1. INTRODUCTION

That our space might have a more complicated texture than conventional three dimensions of infinite (or nearly infinite) size has been suggested a long time ago. The original idea perhaps goes back as far as Bernhard Riemann's famous Habilitation lecture [1] in which he introduced the concepts of what are now known as the Riemannian space and curvature tensor. It was not until the XXth century that these novel ideas have been first employed by physicists: with Albert Einstein's general relativity (GR) theory [2] based on the Riemann's concept of space, and Theodore Kaluza and Oscar Klein's interesting, albeit unsuccessful attempt to unify GR with electromagnetism (EM) by introducing an additional spatial dimension of a finite size [3] (in what follows referred to as a *compact dimension*). In 1970-ies the concept of compact dimensions has been utilized by string theory, that requires additional six or seven very small spatial dimensions (usually with the size  $\sim 10^{-35}$  m) for a self-consistent description of quantum gravity. Unfortunately, such tiny extra dimensions (ED) cannot be probed in any existing or foreseen experiments as the "resolution" necessary to penetrate such small distances would require a center-of-mass energy  $\sim 10^{13}$  TeV, i.e. far beyond the range spanned by either natural or man-made beams. Consequently, these extra dimensions remain more of a mathematical concept than a falsifiable physics prediction, at least for now.

For a particle propagating in the extra dimensions the boundary conditions allow only for certain eigenvalues of energy (cf. classical "particle in a box" problem). These quantized energy states look like a tower of massive particles from the point of view of a 3-dimensional (3D) observer and are referred to as Kaluza-Klein (KK) modes or excitations of a particle. Typical energy spacing between the KK modes is  $\sim 1/R^1$ . As the following discussion will reveal, these KK-modes can modify the conventional picture of physical world in a most profound way.

It was not until 1998 that the idea of extra dimensions in space has been used as a possible solution of the one of the most embarrassing problems of the Standard Model (SM) of particle physics – the hierarchy problem. The essence of this problem can be captured in a single question: why is gravity (at least as we observe it) some  $10^{38}$  orders of magnitude weaker than other forces of Nature? This mysterious fact is responsible for a tremendous hierarchy of energy scales: from the scale of electroweak (EW) symmetry breaking ( $M_{\text{EW}} \sim 1$  TeV) to the energies at which gravity is expected to become as strong as other known forces (strong, EM, and weak), known as Planck scale or  $M_{\text{Pl}} = 1/\sqrt{G_N} = \sim 10^{16}$  TeV, where  $G_N$  is the Newton's coupling constant.

Why is the hierarchy problem so annoying? The reason is that in our everyday experience, large hierarchies tend to collapse, unless they are supported by some intermediate layers or by a certain amount of fine tuning of the initial conditions. E.g., it is mechanically possible to balance a billiard cue on its point, but the amount of fine tuning

---

<sup>\*</sup>On behalf of the CDF and DØ Collaborations.

<sup>†</sup>E-mail: landsberg@hep.brown.edu.

<sup>1</sup>Here and in what follows we use "natural" units  $\hbar = c = 1$ .

required for such a delicate balance is too demanding to be of a practical use. Indeed, walking in a room and seeing a cue standing steadily on its end would be too odd not to suspect a some kind of hidden support. Similarly, making the SM work for all energies up to the Planck scale would require tremendous amount of fine tuning of its parameters – to a precision of  $\sim (M_{\text{Pl}}/M_{\text{EW}})^2 \sim 10^{-32}$ . A natural reaction to this observation is to conclude that the SM is not complete and certain new physics has to exhibit itself at the energies of the order of the EW scale, thus “supporting” the hierarchy with an extra layer.

Nevertheless, it’s worth noting that large amounts of fine tuning, while unnatural, are not prohibited by any fundamental principle. The fact that large hierarchies tend to collapse is merely empirical. While many large hierarchies we know have indeed collapsed (e.g., human towers, once they have too many layers, countless monarchies, the Soviet empire), some others are surprisingly stable (e.g., Egyptian pyramids, Eiffel tower, George W. Bush’s government). Note also that certain examples of fine tuning have been observed in Nature:

- One of the best known examples of fine tuning is the fact that the apparent angular size of the moon is the same as the angular size of the Sun within 2.5% – a mere coincidence to which we owe such a spectacular sight as solar eclipse.
- Somewhat less abused example is the infamous Florida 2000 presidential election recount with the official result of 2,913,321 Republican vs. 2,913,144 Democratic votes, with the ratio equal to 1.000061, i.e. fine-tuned to one with the precision of 0.006%.
- Yet less known example<sup>2</sup> is that the ratio of 987654321 to 123456789 is equal to 8.000000073, i.e. eight with the precision of  $9.1 \times 10^{-9}$ .

## 2. EXTRA DIMENSIONS AND THE HIERARCHY PROBLEM

The first attempt to solve the hierarchy problem using extra spatial dimensions was made by Nima Arkani-Hamed, Savas Dimopoulos, and Georgi Dvali (ADD) [4]. The idea was drastically different from the common utilization of extra dimensions in string theory. In the ADD paradigm extra spatial dimensions are used to create an extra volume, which is sufficiently large to dilute gravity, so that it appears weak to a 3D-observer. To realize this the extra dimensions have to be many orders of magnitude larger than those in string theory. In order for such “large” extra dimensions not to violate any constraints from atomic physics and other experimental data, all other particles except for the graviton must not be allowed to “feel” the extra space. Fortunately, modern quantum field theory allows to confine spin 0, 1/2, and 1 particles to a subset of a multidimensional space, or a “brane.” At the same time, the graviton, being a spin-2 particle, is not confined to the brane and thus penetrates the entire (“bulk”) space. The solution to the hierarchy problem (or rather its “removal”) then becomes straightforward: if the Planck scale in the multidimensional space is of the order of the EW scale, then there is no large hierarchy and no fine-tuning problem to deal with, as non-trivial physics really “ends” at the energies  $\sim 1$  TeV. Gravity appears weak to a 3D-observer merely because it spans the entire bulk space; therefore the gravitons spend very little time in the vicinity of our brane. Gravity in 3D is literally diluted by the enormous volume of extra space.

The size of large extra dimensions ( $R$ ) is fixed by their number ( $n$ ) and the *fundamental* Planck scale in the  $(4+n)$ -dimensional space-time ( $M_D$ ). By applying Gauss’s law, one finds [4, 6]:

$$M_{\text{Pl}}^2 = 8\pi M_D^{n+2} R^n. \quad (1)$$

---

<sup>2</sup>This happens to be not just a mere coincidence, but actually an example of a certain “hidden” principle that guarantees large amount of fine tuning. In this example, it turns out that in the base- $N$  numerical system the ratio of the number composed of digits  $N-1$  through 1 in the decreasing order to the number obtained from the same digits, placed in the increasing order, is equal to  $N-2$  with the precision asymptotically approaching  $10^{-N}$ . Playing with a hexadecimal calculator could easily reveal this via the observation that the ratio of FEDCBA987654321 to 123456789ABCDEF is equal to 14.000000000000000183, i.e. 14 with the precision of  $1.3 \times 10^{-17}$ . Whether the  $10^{-38}$  precision needed to fine-tune the SM could be a result of a similarly hidden principle is yet to be found out.

(Here for simplicity we assumed that all  $n$  dimensions have the same size  $R$  and are compactified on a torus.)

If one requires  $M_D \sim 1$  TeV and a single extra dimension, its size has to be of the order of the radius of the solar system; however, already for two ED their size is only  $\sim 1$  mm; for three ED it is  $\sim 1$  nm, i.e. similar to the size of an atom; and for larger number of ED it further decreases to subatomic sizes and reaches  $\sim 1$  fm (the size of a proton) for seven ED.

A direct consequence of these compact extra dimensions in which gravity is allowed to propagate, is a modification of Newton's law at the distances comparable with the size of ED: the gravitational potential would fall of as  $1/r^{n+1}$  for  $r \lesssim R$ . This clearly rules out the possibility of a single ED, as the very existence of our solar system requires the potential to fall of as  $1/r$  at the distances comparable with the size of planetary orbits. However, it turns out that as of 1998 any higher number of ED have not been ruled out by any gravitational measurements, as Newton's law has not been tested to the distances smaller than about 1 mm. Amazing as it is, large ED with the size as macroscopic as 1 mm were perfectly consistent with the host of experimental measurements at the time when the ADD idea has appeared!

Note that the solution to the hierarchy problem in the ADD paradigm is incomplete. In a sense, the hierarchy of energy scales is traded for the hierarchy of distances from a "natural" electroweak symmetry breaking (EWSB) range of  $1 \text{ TeV}^{-1} \sim 10^{-19} \text{ m}$  to the much larger size of the compact extra dimensions. Nevertheless, this hierarchy could be significantly smaller than the hierarchy of energy scales or perhaps stabilized by some topological means. Strictly speaking, the idea of large extra dimensions is really a paradigm which can be used to build more or less realistic models, rather than a model by itself.

Almost simultaneously with the ADD paradigm a very different low-energy utilization of the idea of compact extra dimensions has been proposed by Keith Dienes, Emilian Dudas, and Tony Gherghetta [7]. In their model, additional dimension(s) of the "natural" EWSB size of  $R \sim 1 \text{ TeV}^{-1}$  [8] are added to the SM to allow for a low-energy unification of gauge forces. In conventional SM and its popular extensions, such as supersymmetry, gauge couplings run logarithmically with energy, which is a direct consequence of the renormalization group evolution (RGE) equations. Given the values of the strong, EM, and weak couplings at low energies, all three couplings are expected to "unify" (i.e., reach the same strength) at the energy  $\sim 10^{13} \text{ TeV}$ , known as the Grand Unification Theory (GUT) scale. However, if one allows gauge bosons responsible for strong, EM, and weak interactions to propagate in extra dimensions, the RGE equations would change. Namely, once the energy is sufficient to excite KK modes of gauge bosons (i.e.  $\sim 1/R \sim 1 \text{ TeV}$ ), running of the couplings is proportional to a certain power of energy, rather than its logarithm. Thus, the unification of all three couplings can be achieved at much lower energies than the GUT scale, possibly as low as 10-100 TeV [7].

An obvious deficiency of this model is that it does not incorporate gravity and thus does not explain its weakness relative to other forces. Nevertheless, it removes another hierarchy of a comparable size – the hierarchy between the EWSB and GUT scales<sup>3</sup>.

In 1999, Lisa Randall and Raman Sundrum offered a rigorous solution [9] of the hierarchy problem by adding a single extra dimension (with the size that can range anywhere from  $\sim 1/M_{\text{Pl}}$  virtually to infinity) with a non-Euclidean, warped metric. They used the Anti-deSitter (AdS) metric (i.e. that of a space with a constant negative curvature)  $ds^2 = \exp(-2kR|\varphi|)\eta_{\mu\nu}dx^\mu dx^\nu - R^2d\varphi^2$ , where  $0 \leq \varphi < 2\pi$  is the coordinate along the extra spatial dimension of radius  $R$ ,  $k$  is the curvature of the AdS space (warp factor),  $x^\mu$  are the conventional (3+1)-space-time coordinates, and  $\eta^{\mu\nu}$  is the metric of the Minkowski space-time. A (3+1)-dimensional brane with positive tension is put at  $\varphi = 0$ . If gravity originates on this brane (Planck brane), the wave function of the graviton has a peculiar feature that it is exponentially suppressed away from the brane in the direction of the extra dimension. If all the SM fields were confined to the Planck brane, one would not have seen any low-energy effects in this model. However, if a second brane with negative tension (SM brane) is put at  $\varphi = \pi$ , than the  $M_{\text{Pl}}$ -size operators on the Planck

---

<sup>3</sup>Since we don't understand gravity at the quantum level, it's not clear what would happen to the running of the gravitational coupling if a graviton is allowed to propagate in  $\text{TeV}^{-1}$  ED.

brane would result in low-energy effects on the SM brane with the typical scale of  $\Lambda_\pi = \overline{M}_{\text{Pl}} \exp(-k\pi R)$ , where  $\overline{M}_{\text{Pl}} \equiv M_{\text{Pl}}/\sqrt{8\pi}$  is the reduced Planck mass. If the SM fields are confined to the SM brane, the hierarchy problem is solved for  $\Lambda_\pi \sim 1$  TeV, which can be achieved with a little amount of fine tuning by requiring  $kR \sim 10$ . Since the only fundamental scale in this model is  $M_{\text{Pl}}$ , the hierarchy problem is solved naturally for  $R \sim 1/M_{\text{Pl}}$ . It is even possible to stabilize the Planck and SM branes at  $\varphi = 0$  and  $\pi$ , respectively, by putting them in the fixed points of an orbifold in the AdS space.

In the simplest Randall-Sundrum (RS) model [9], gravitons are the only particles propagating in the AdS space. Several extensions of this model exist [10], where various other particles are allowed to propagate in the bulk space, leading to rich low-energy phenomenology.

Another interesting feature of the RS model is the existence of a new, Higgs-like scalar particle, the radion which is a modulus field describing relative motion of the two branes [11]. Radion phenomenology has been a subject of intense theoretical studies in the past few years [12]. Particularly interesting is the Higgs-radion mixing, which would modify the branching fractions of the standard model Higgs, thus affecting the sensitivity of collider searches for the Higgs boson. Similar to the Higgs searches, high energy and integrated luminosity are the keys to the radion searches at colliders. However, in the allowed and theoretically preferred parameter space of the RS model it is very unlikely that the radion can be observed at the Tevatron, so a more detailed discussion of its phenomenology goes beyond the scope of this paper.

The most “democratic” of the ED models has been suggested in 2000 by Thomas Appelquist, Hsin-Chia Cheng, and Bogdan Dobrescu and is referred to as universal extra dimensions (UED) [13]. In this model, all the SM particles are allowed to propagate in the bulk space of several extra dimensions of a  $\text{TeV}^{-1}$  size. A special quantum number, the Kaluza-Klein parity, is conserved in this model:  $n_1 \pm n_2 \pm n_3 \pm \dots \pm n_N = \text{const}$ , where  $n_i$  is the Kaluza-Klein mode for the  $i$ -th particle of a certain multiparticle state. One of the consequences of this conservation law is that if one produces a final state of  $N$  particles in collisions of the 0-th KK modes (e.g., at colliders), the Kaluza-Klein parity of the final state has to remain zero, which implies that one can not produce a single excited KK mode in such a collision. Consequently, as in SUSY with  $R$ -parity conservation, excited KK modes must be produced in pairs, which lifts many would-be constraints on the UED model. Another consequence is that the lightest KK excitation (LKKE) – that of a photon – must be stable and provides a suitable candidate for the cold dark matter [14]. Radiative corrections to the KK spectrum of SM particles break mass degeneracy between KK excitations of various particles and result in SUSY-like cascade decays terminated with a pair of LKKE’s in the final state, which could be even confused for a SUSY spectrum at the LHC and future colliders [15]. While UED offer a number of interesting low-energy effects, there are no results on the UED searches at the Tevatron as of yet. Consequently, we won’t discuss this model in any more detail here.

To summarize, various new models with extra dimensions can solve some of the deficiencies of the SM. While inspired by string theory, none of these models are based on it. Note that in principle several of the models can be realized in Nature simultaneously. For example, one could imagine a universe with six extra dimensions, three of which are large, one has a  $\text{TeV}^{-1}$  size, and two others are of a very small radius expected naturally in string theory. Thus, string theory, low energy GUT, and TeV-scale gravity might in principle all coexist!

Finally, in 2002 yet another class of models based on ED has been suggested by Nima Arkani-Hamed, Andy Cohen, and Howard Georgi. In these models the concept of extra dimensions is used to build a multi-dimensional theory, which at the end of the day looks like a 4-dimensional one [16]. There exist interesting implementations of this class of models [17], in which the hierarchy problem is solved by introducing an additional scale  $\sim 100$  TeV and a light Higgs boson (little Higgs) responsible for EWSB. Quadratic divergencies of the SM are cancelled up to this new scale by additional vector-like quarks. These models predict moderate low-energy phenomenology and typically require a few additional particles with masses  $\sim 1$  TeV, particularly an extra neutral massive gauge boson  $Z_H$  with the properties similar to those of the  $Z$ .

### 3. PROBING EXTRA DIMENSIONS IN THE LAB

The most experimentally-interesting feature of recent ED models is rich low-energy phenomenology that originates from the KK spectrum of various particles propagating in ED. In what follows we compare the KK spectrum observed in the ADD,  $\text{TeV}^{-1}$ , and RS models and discuss various experimental constraints on model parameters.

#### 3.1. Kaluza-Klein Spectrum and Low-Energy Phenomenology

In the ADD model, the only particle that propagates in ED and acquires KK modes is the graviton. Given the size of ED ( $\sim 10^{-3}\text{--}10^{-15}$  m), energy spacing between the KK excitations of the graviton is  $\sim 1 \text{ meV} - 100 \text{ MeV}$ . Consequently, the adjacent modes are hard to resolve and in most of the experiments the KK spectrum would appear continuous, from zero to a certain ultraviolet cutoff above which quantum gravity effects would modify this semi-classical picture. Since the fundamental Planck scale in the ADD model is  $M_D \sim 1 \text{ TeV}$ , it's natural to expect this cutoff,  $M_S$ , to be of the same order:  $M_S \sim M_D$ . While each KK mode couples to the energy-momentum tensor with gravitational strength  $G_N$ , the sheer number of available KK modes is sufficient to enhance gravitational attraction tremendously. For example, in a particle collision with the energy  $\sim 1 \text{ TeV}$  as many as  $10^4$  KK modes along each extra dimension are accessible, even in the case of the smallest radius of these ED,  $\sim 1 \text{ fm}$ . Given that this size corresponds to  $n = 7$ , a total of  $10^{4n} = 10^{28}$  modes can be excited, thus magnifying gravitational interaction by this enormous factor.

In the  $\text{TeV}^{-1}$  model with a single extra dimension of the size  $R$ , the 0-th KK mode of a gauge boson is the SM particle of mass  $M_V$ . This mass can be either 0 (photon, gluon) or  $> 0$  ( $W, Z$ ). The mass of the  $i$ -th KK mode is given by the following equation:

$$M_i = \sqrt{M_V^2 + i^2/R^2}. \quad (2)$$

For the compactification scale  $M_C \equiv 1/R \sim 1 \text{ TeV}$ ,  $1/R \gg M_V$  and hence KK modes of all gauge bosons are nearly degenerate. Consequently, the mass of the  $i$ -th mode is approximately equal to  $iM_C$  for any  $i > 0$ . The couplings of all the KK modes of gauge bosons with  $i > 0$  to the SM fields are  $\sqrt{2}$  greater than the couplings of the corresponding SM bosons. This factor comes from the normalization of the KK modes (due to the fact that the negative values of  $i$  are not considered and only the positive ones are kept in the effective Lagrangian). While the graviton, which is presumably free to propagate in the entire bulk space, would also acquire KK modes with the energy spacing  $M_C$ , these modes are sufficiently sparse not to affect gravitational interaction by a visible amount. For example, if the energy of an interaction is as high as 100 TeV, the gravitational interaction is increased just by two orders of magnitude, i.e. imperceptibly small. The KK tower of excited gauge bosons is expected to be truncated at the masses of the order of the new GUT scale (i.e.,  $\sim 100 \text{ TeV}$ ), where new physics (e.g., brane dynamics) should take over.

Finally, in the Randall-Sundrum model the 0-th KK mode of the graviton remains massless, while the higher modes have masses spaced as subsequent zeros of the Bessel's function  $J_1$ . Such an "exotic" solution comes from the fact that the graviton is confined to a "box" with a peculiar warped metric. On the other hand, an observation of just two excitations of the KK graviton with the ratio of the masses being at a zero of  $J_1$  would be a unique smoking-gun signature of warped extra dimensions. If the mass of the first excited mode of the graviton is  $M_1$ , the subsequent excitations would have masses of  $1.83M_1, 2.66M_1, 3.48M_1, 4.30M_1$ , etc. The spacing between the subsequent KK excitations decreases at high masses. The 0-th excitation is coupled to the energy-momentum tensor with gravitational strength  $G_N$ , while each of the higher excitations couples with the strength  $\sim 1/\Lambda_\pi^2$ , i.e. comparable with the EW coupling strength. The excited modes are presumably truncated at masses  $\sim M_{\text{Pl}}$ , where brane excitations would modify the discussed behavior.

### 3.2. Direct Gravity Measurements

The most straightforward observable effect of the large ED is the modification of Newton's gravitational attraction law at very short distances. Current and forseen techniques only allow these measurements to probe extra dimensions as small as  $\sim 50 \mu\text{m}$ , which limits their applicability to the case of  $n = 2$ , assuming that all ED have similar sizes. However, since the relationship between the fundamental and apparent Planck scales depends only on the total volume of extra space, and not on the shape of extra dimensions, it is possible that even for higher number of extra dimensions, one of them could be macroscopic, while the other ones are much smaller. Since gravity measurements are sensitive to the largest extra dimension, they can probe such asymmetric cases even for  $n > 2$ . Unfortunately, gravity measurements at short distances offer no sensitivity to the  $\text{TeV}^{-1}$  and RS models.

Currently, the best limit on the size of extra dimensions in the ADD model from gravity measurements comes from the Eöt-Washington group [18] and constrains the largest ED size to  $R < 0.16 \text{ mm}$  at the 95% confidence level (CL), which corresponds to  $M_D > 1.7 \text{ TeV}$  in the case of two ED of equal size. For further discussion of the "tabletop" gravitational experiments, see Sylvia Smullin's talk at SSI '04 [19] or Ref. [20].

### 3.3. Constraints from Astrophysics and Cosmology

Certain constraints on the ADD model come from astrophysical observations and cosmology. For example, KK graviton ( $G_{\text{KK}}$ ) emission could serve as an alternative cooling mechanism for the supernovae, thus suppressing the dominant SM mechanism – the neutrino emission. The observation of a handful of neutrinos from the SN1987A explosion by the IMB and Kamiokande detectors allowed to put a constraint of  $M_D > 25\text{--}30 \text{ TeV}$  for  $n = 2$  and  $2\text{--}4 \text{ TeV}$  for  $n = 3$  [21]. For any higher number of ED limits on  $M_D$  are below 1 TeV. Other constraints come from non-observation of a distortion of cosmic diffuse gamma-radiation spectrum expected from the decays of KK gravitons into pairs of photons [22] and from the lack of photon emission from the decays of gravitons trapped in the vicinity of neutron stars formed in the process of supernovae collapse [23]. A significant excess of KK gravitons in early universe would result in its overclosure or early matter dominance, which also leads to constraints [24] on  $M_D$ .

All these limits have similar features: they are typically rather strong (up to 1700 TeV!) for  $n = 2$ , moderate (a few TeV) for  $n = 3$ , and rather weak for  $n > 3$ . The other feature of these constraints is that all of the underlying calculations are based on a number of assumptions, so the results are reliable only as an order of magnitude estimate. (It is not unusual for different calculations based on the same data to differ by a factor of 2–3.) Nevertheless,  $n = 2$  case seems to be largely disfavored by the host of the astrophysical and cosmological constraints.

None of the astrophysical or cosmological arguments result in any important limits on the  $\text{TeV}^{-1}$  or RS models. Further review of constraints from astrophysics and cosmology can be found in Ref. [25].

### 3.4. Collider Constraints on Extra Dimensions

High-energy colliders are the finest microscopes invented by the human kind. The discovery of the top quark at Fermilab [26] showed that distances as small as  $10^{-18} \text{ m}$  can be probed effectively. Hence, they remain ultimate tools in probing large extra dimensions for virtually any value of  $n$ .

Since the KK gravitons couple to the energy-momentum tensor, they can be added to any vertex or line of the SM Feynman diagram. Consequenly, to probe ADD model at colliders one could either look for direct emission of KK gravitons, e.g. in the  $q\bar{q}' \rightarrow g + G_{\text{KK}}$  process, which result in a single jet (monojet) in the observable final state, or an apparent transverse momentum non-conservation and overall enhancement of the SM monojet spectrum at high jet energies. Another type of effect observable in high-energy collisions is an enhancement of Drell-Yan (DY) or diboson spectrum at high invariant masses due to additional diagrams involving virtual KK graviton exchange. Typically, these diagram interfere with their SM counterparts, as shown in Fig. 1 for the case of DY production.

Virtual graviton effects are complementary to those of direct graviton emission, since the former depend on the ultraviolet cutoff of the KK spectrum,  $M_S$ , while the former depend directly on the fundamental Planck scale  $M_D$ . While both scales are expected to be of the same order, it is quite possible that  $M_S$  is somewhat lower than  $M_D$ ; thus

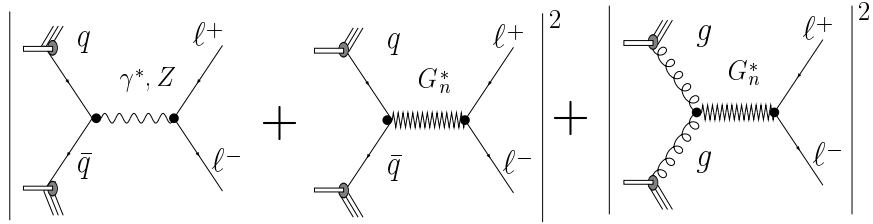


Figure 1: Feynman diagrams for modified DY production in the presence of large extra dimensions. From Ref. [27].

the effects of extra dimensions might show up in the virtual graviton exchange before they are observed in the direct emission. While the direct graviton emission cross section is well defined [6, 28], the cross section for virtual graviton exchange depends on the particular representation of the interaction Lagrangian. Three such representations have appeared nearly simultaneously [6, 29, 30]. In all three of them, the effects of ED are parameterized via a single variable  $\eta_G = \mathcal{F}/M_S^4$ , where  $\mathcal{F}$  is a dimensionless parameter of order unity, reflecting the dependence of virtual  $G_{KK}$  exchange on the number of extra dimensions and  $M_S$  is the ultraviolet cutoff. Different formalisms use different definitions of  $\mathcal{F}$ :

$$\mathcal{F} = 1, \text{ (GRW [6]);} \quad (3)$$

$$\mathcal{F} = \begin{cases} \log\left(\frac{M_S^2}{M^2}\right), & n = 2 \\ \frac{2}{n-2}, & n > 2 \end{cases}, \text{ (HLZ [30]);} \quad (4)$$

$$\mathcal{F} = \frac{2\lambda}{\pi} = \pm \frac{2}{\pi}, \text{ (Hewett [29]).} \quad (5)$$

Note that only within the HLZ formalism  $\mathcal{F}$  depends explicitly on  $n$ . In both the GRW and HLZ formalisms gravity effects interfere constructively with the SM diagrams. In Hewett's convention the sign of interference is not known, and it's parameterized via a parameter  $\lambda$  of order unity, which is usually taken to be either +1 (constructive interference) or -1 (destructive interference). The parameter  $\eta_G$  has dimensions of  $\text{TeV}^{-4}$  with  $M_S$  in units of  $\text{TeV}$ , and describes the strength of gravity in the presence of large ED. The differential or total cross section in the presence of virtual graviton exchange can be parameterized as:

$$\sigma_{\text{tot}} = \sigma_{\text{SM}} + \eta_G \sigma_{\text{int}} + \eta_G^2 \sigma_G, \quad (6)$$

where  $\sigma_{\text{SM}}$  is the SM cross section for the process under study and  $\sigma_{\text{int}}$ ,  $\sigma_G$  are the interference and direct graviton effects, respectively.

The most dramatic and exciting observable effect of large ED is copious production of black holes at future accelerators with the c.o.m. energy exceeding the fundamental Planck scale [31] (e.g., at the LHC) and in ultra-high-energy cosmic-ray interactions [32]. This topic goes beyond current Tevatron sensitivity and is covered in separate reviews [33].

LEP experiments pioneered searches for extra dimensions at colliders in both direct graviton emission in the  $e^+e^- \rightarrow \gamma/Z + G_{KK}$  mode and via virtual graviton exchange in the DY production of various fermion pairs, as well as in the diboson production. The best sensitivity is achieved in the  $e^+e^- \rightarrow \gamma G_{KK}$  and in the  $e^+e^- \rightarrow e^+e^-, \gamma\gamma$  modes. The preliminary individual and combined LEP limits from direct graviton emission process are listed in Table I [34]. Here and in what follows, all limits are quoted at the 95% CL.

Combined LEP limit on  $M_S$  from di fermion and diphoton production in Hewett's convention is 0.95 TeV (destructive interference) or 1.14 TeV (constructive interference) [35].

Both CDF and DØ Collaboration at the Fermilab Tevatron  $p\bar{p}$  collider sought for large ED in Run I. DØ has pioneered a search in the dielectron and diphoton channels at hadron colliders [36], as well as a search in the challenging monojet channel [37] plagued by large instrumental backgrounds from jet mismeasurement and cosmics. CDF has pioneered search in the monophoton channel at hadron colliders [38] and also accomplished a monojet analysis [39]. DØRun I limits on the virtual graviton effects in Hewett's convention are  $M_S > 1.0$  and 1.1 TeV for

Table I: Individual and combined 95% CL limits on the fundamental Planck scale  $M_D$  in the large ED model (in TeV) from the LEP experiments. OPAL limits are based only on the 1998  $\sqrt{s} = 189$  GeV data and are not used in the combination.

Experiment	$n = 2$	$n = 3$	$n = 4$	$n = 5$	$n = 6$
ALEPH	1.26	0.95	0.77	0.65	0.57
DELPHI	1.31	1.02	0.82	0.67	0.58
L3	1.50	1.14	0.91	0.76	0.65
OPAL	1.09	0.86	0.71	0.61	0.53
Combined (ADL)	1.60	1.20	0.94	0.77	0.66

the negative and positive interference signs, respectively. (These limits are the tightest limits on  $M_S$  coming from a single experiment.)

The results of the monojet and monophotons searches in Run I are summarized in Table II. The unknown next-to-leading order corrections are parameterized via a constant K-factor and the limits are given at the leading order  $K = 1$  and for  $K = 1.3$ , typical for many production processes at the Tevatron.

Table II: Individual 95% CL limits on the fundamental Planck scale  $M_D$  in the large ED model (in TeV) from the CDF and DØ experiments. Ordering of the results is chronological.

Experiment and channel	$n = 2$	$n = 3$	$n = 4$	$n = 5$	$n = 6$	$n = 7$	$n = 8$
CDF monophotons, $K = 1$			0.549		0.581		0.602
DØ monojets, $K = 1$	0.89	0.73	0.68	0.64	0.63	0.62	
DØ monojets, $K = 1.3$	1.99	0.80	0.73	0.66	0.65	0.63	
CDF monojets, $K = 1$	1.00		0.77		0.71		
CDF monojets, $K = 1.3$	1.06		0.80		0.73		

HERA experiments have also looked at the effects of the  $t$ -channel exchange of virtual gravitons in the  $ep \rightarrow ep$  data and set limits on the ultraviolet cutoff  $M_S$  of 0.82 and 0.79 TeV in Hewett's convention for constructive and destructive interference, respectively [40].

As of beginning of Run II, there have been no dedicated searches for  $\text{TeV}^{-1}$  extra dimensions. However, a number of constraints have been derived by phenomenological analysis of the existing data. For a review of indirect constraints see, e.g. Ref. [41]. The best limits come from the analysis of the LEP precision measurements; the combined limits on the compactification scale of the  $\text{TeV}^{-1}$  dimensions  $M_C \equiv 1/R$  reach 6.8 TeV.

Finally, as of the beginning of Run II there have been virtually no experimental constraints on Randal-Sundrum extra dimensions or Little Higgs models. The only existing ones come from precision electroweak observables and are rather weak.

## 4. Recent Tevatron Searches for Extra Dimensions

Past year has been extremely successful for the Tevatron collider and the CDF and DØ experiments. After lagging behind for a while, hot only the instantaneous luminosity has achieved the design level, and actually exceeded it. A record luminosity of  $1.0 \times 10^{32}$  has been achieved in the most luminous store to date, which happened June , 2004. Both CDF and DØ Collaborations have logged nearly  $0.5 \text{ fb}^{-1}$  of physics data since the beginning of Run II in 2001, of which  $\approx 60\%$  came last year. Both experiments function very efficiently with the average data-logging efficiency of 85% over the last year. Most of the analyses presented in this paper are based on approximately half of the total recorded data set. The next update based on full recorded statistics is expected in early 2005.

Table III: 95% C.L. lower limits (in TeV) on the compactification scale  $M_C \equiv 1/R$  of the  $\text{TeV}^{-1}$  ED. From Ref. [41].

Experiment and channel	$M_C^{95}$ (TeV)
LEP 2:	
hadronic cross section, angular distributions, $R_{b,c}$	5.3
$\mu, \tau$ cross section, angular distributions	2.8
$ee$ cross section, angular distributions	4.5
LEP combined	6.6
HERA:	
$ep \rightarrow e + X$	1.4
$ep \rightarrow \nu + X$	1.2
HERA combined	1.6
TEVATRON:	
Drell-Yan	1.3
Dijet production	1.8
Top production	0.60
Tevatron combined	2.3
All combined	6.8

#### 4.1. DØ Search for Large Extra Dimensions in the Monojet Channel

The monojet channel offer the best direct sensitivity to the fundamental Planck scale at the Tevatron. As was shown in the previous section, its sensitivity is superior to that in the monophoton channel. Nevertheless, it is a very challenging channel experimentally, since there are copious instrumental backgrounds, which have to be understood and suppressed<sup>4</sup>. Apart from instrumental background, there is an irreducible physics background from  $Z(\nu\nu) + \text{jet}$  production, which require stringent cutoffs on jet transverse energy ( $E_T$ ) and missing transverse energy ( $\cancel{E}_T$ ), which is a characteristic signature of the graviton escaping in the bulk space.

Recently DØ has produced the first preliminary result of searches for large ED in the monojet channel based on new data collected in Run II of the Tevatron. This analysis corresponds to an integrated luminosity on  $85 \text{ pb}^{-1}$  collected with a special hardware trigger that required the vector sum of transverse energies of jets to exceed 20 GeV. The analysis is based on a subset of the available data collected with this trigger and should be really considered as a proof-of-principle, or a warm-up exercise to a more sensitive analysis based on large statistics. Nevertheless, even with this small subset of data an impressive sensitivity has been achieved. Offline, both jet  $E_T$  and  $\cancel{E}_T$  are required to exceed 150 GeV and a number of quality cuts are introduced to reduce backgrounds. No additional jets with the  $E_T > 50$  GeV are required in the event and the direction of  $\cancel{E}_T$  is required to be at least  $30^\circ$  away in azimuth from any jet in the event. That leaves 63 candidate events (from the initial sample of 360K events) and corresponds to typical signal efficiency  $\sim 5\%$ , mainly due to high  $E_T$  and  $\cancel{E}_T$  cuts. The number of candidate events agrees within the errors with the expected background of  $100 \pm 9^{+50}_{-30}$  events, where the second uncertainty is due to the dominant systematics related to the jet energy scale (JES). The background is dominated by the irreducible  $Z(\nu\nu) + \text{jets}$  background, with the second most important contribution coming from the  $W(\tau\nu) + X$  production where  $\tau$  is either missed or reconstructed as a jet. The  $E_T$  spectrum of the leading jet is shown in Fig. 2.

Since the data agree with predicted background, limits on large ED are set. The signal is simulated with PYTHIA [42] Monte Carlo with the large ED effects implementation of Ref. [43], followed by a full simulation of the DØ detector. Uncertainty on the JES is the dominant systematics for the signal. Limits on the fundamental

<sup>4</sup>As an evidence of experimental challenge, it's worth noting that it took both the CDF and DØ experiments some four years to complete the monojet analyses in Run I.

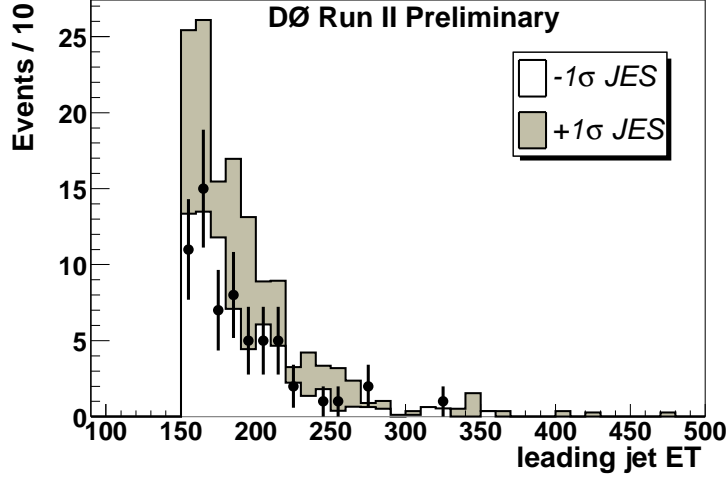


Figure 2: Transverse energy of the leading jet in the DØ Run II monojet analysis. Points are data, histogram is the expected background, with the shadow band corresponding to the change in the JES of  $\pm$  one standard deviation.

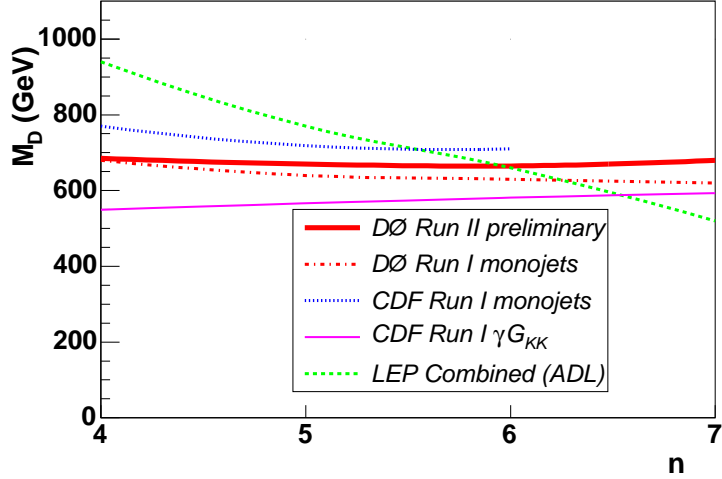


Figure 3: Limits on the fundamental Planck scale  $M_D$  from the DØ monojet analysis in Run II. Also shown are the Tevatron Run I ( $K = 1$ ) and LEP limits.

Planck scale  $M_D$  from this analysis (for the  $K$ -factor of 1) are listed in Table IV and shown in Fig. 3, together with the Tevatron Run I and LEP constraints. Note that they already improve on the DØ Run I limits, although are still shy of the CDF Run I limits. It's worth mentioning that the Tevatron and LEP searches are complementary: Tevatron has higher sensitivity for high number of ED  $n$ , while LEP offers better limits for small  $n$ .

Table IV: Individual 95% CL limits on the fundamental Planck scale  $M_D$  in the large ED model (in TeV) from the DØ Run II analysis.

$n = 4$	$n = 5$	$n = 6$	$n = 7$
0.68	0.67	0.66	0.68

Since the analysis has been completed, the JES systematics has been reduced by a factor of two. Together with much higher statistics recorded with the new trigger, the next update of the DØ analysis expected in early 2005 should reach new level of sensitivity to large ED and supersede previous Tevatron and LEP results.

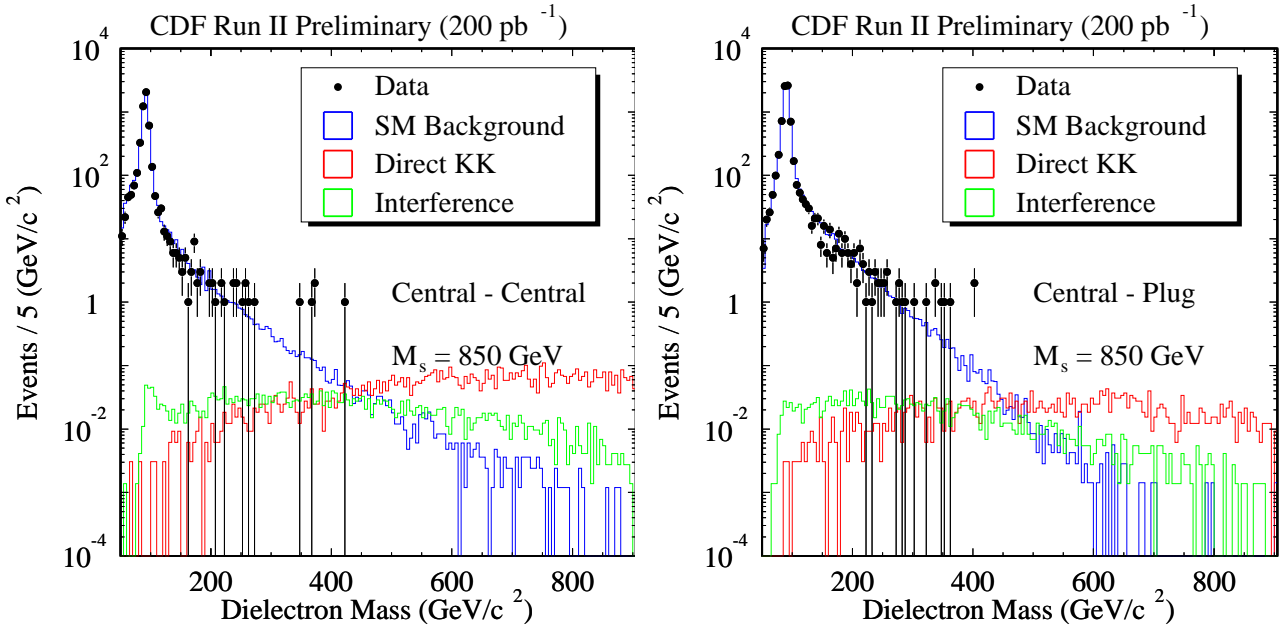


Figure 4: Dielectron mass spectrum from the CDF search for large extra dimensions via virtual graviton effects. Left: central-central; right: central-forward combinations. Points are data; solid line is the sum of SM backgrounds. Also shown in the plots is the contribution from the interference and direct term for  $M_S = 850$  GeV (in Hewett's convention).

#### 4.2. Searches for Large Extra Dimensions via Virtual Graviton Effects

Both Tevatron collaboration pursue search for large ED in Drell-Yan and diphoton production in Run II. Recent CDF analysis is based on  $200 \text{ pb}^{-1}$  of dielectron data. Both electrons require to have large transverse energy and satisfy standard quality criteria. At least one of the electrons is required to be in the central region of the detector (i.e.,  $|\eta| < 1.0$ , where  $\eta$  is pseudorapidity measured relative to the center of the detector). The second electron can be either central or forward ( $1.1 < |\eta| < 2.8$ ).

The invariant mass spectra of the dielectrons for two different topologies are shown in Fig. 4. They agree well with the expected background dominated by the DY production. The shape of the contributions from virtual graviton exchange for  $M_S = 850$  GeV (in Hewett's convention) are also shown in the figure. As seen from the plot, the dominant contribution in the region where signal exceeds expected background is from the direct gravity term (see Eq. (6), rather than the interference term. Given no evidence for large ED, limits on the ultraviolet cutoff  $M_S$  are set within different formalisms and are listed in Table V. A LO event generator from Ref. [44] has been used to generate signal, with next-to-leading order effects on the signal accounted for via a constant  $K$ -factor of 1.3, similar to that for DY – the choice which has been recently justified by exact next-to-leading order calculations for virtual graviton production and decay into a lepton pair [45].

Experiment	GRW [6]						HLZ [30]		Hewett [29]	
	$n=2 \ n=3 \ n=4 \ n=5 \ n=6 \ n=7$						$\lambda = +1$	$\lambda = -1$		
CDF Run II	1.06		1.32	1.11	1.00	0.93	0.88	0.99	0.96	
D $\emptyset$ Run II	1.36	1.56	1.61	1.36	1.23	1.14	1.08	1.22	1.10	
D $\emptyset$ Run I + Run II	1.43	1.67	1.70	1.43	1.29	1.20	1.14	1.28	1.14	

Table V: Lower limits at the 95% CL on the ultraviolet cutoff  $M_S$ , in TeV, from the Tevatron, within several phenomenological frameworks. NLO QCD effects have been accounted for via a  $K$ -factor of 1.3.

The D $\emptyset$  analysis is also based on  $200 \text{ pb}^{-1}$  of data utilizes both diphotons and dielectron channels. In order to maximize the selection efficiency, electrons are not distinguished from photons as the tracking information is not used.

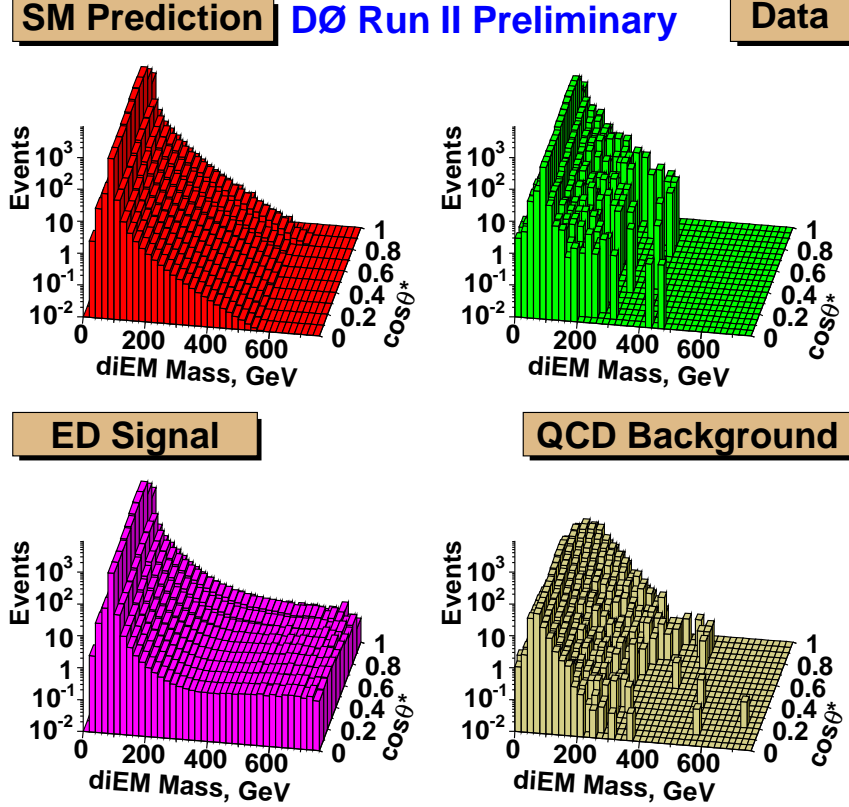


Figure 5: The diEM mass vs.  $\cos \theta^*$  distribution for the DØ diEM candidate sample. Top left: SM background from Drell-Yan and direct diphotons; top right: data; bottom left: ED signal plus the SM background for  $\eta_G = 2.0$ ; bottom right: instrumental background.

This allows one not to lose the events in which one of the photons converted or one of the electrons does not have a reconstructed track. In what follows, we will call such electrons or photons, reconstructed in the calorimeter as “EM objects.” Like in the CDF case, one of the EM objects is required to be central ( $|\eta| < 1.1$ ), while the other one can be either central or forward ( $1.5 < |\eta| < 2.4$ ).

Another important technique used by DØ is the two-dimensional fits in the  $(M_{\text{EM-EM}}, |\cos \theta^*|)$ -plane, where  $\theta^*$  is the scattering angle in the c.o.m. frame. These two variables define the  $2 \rightarrow 2$  pair-production process completely and thus contain full information about the interaction Lagrangian, which allows to achieve maximum sensitivity to gravity effects.

Backgrounds in this search are the SM DY and direct diphoton production, as well as instrumental background from jets misidentified as EM objects. The latter is determined from data by inverting quality cuts on EM objects.

The comparison of the DØ data with the expected SM and instrumental backgrounds, as well as the ED effects in shown in Fig. 5. Note that the SM tail at high values of  $|\cos \theta^*|$  and high masses (due to the collinear divergence in the diphoton production), which would result in decreased sensitivity to large ED effects if only the mass variable is used, does not affect the sensitivity of the 2D-method, as the effects of virtual graviton exchange are most pronounced at high masses and lower values of the  $|\cos \theta^*|$ .

The signal and SM backgrounds are modeled via a LO Monte Carlo generator of Ref. [46], augmented with a fast parameteric simulation of the DØ detector, which takes into account  $p_T$ -boost of the diEM system due to initial state radiation, detector resolutions, and other instrumental effects. Next-to-leading order effects for both signal and SM backgrounds are accounted for via constant  $K$ -factor of 1.3.

Since the data agrees with the sum of instrumental and SM backgrounds, limits on  $M_S$  are set using the template method via a fit to a 2D-analog of Eq. (6). The SM, interference, and direct terms are calculated as 2D-templates in

the  $(M_{\text{EM-EM}}, |\cos \theta^*|)$ -plane and the data is fit to the Eq. (6), bilinear in  $\eta_G$ , which is kept a free parameter of the fit.

The limits obtained as a result of the fit are listed in Table V. These are the most stringent limits on large ED to date, which can be further improved by combining them with the DØ Run I limits [36], as detailed in Table V. Note that for  $n = 2$  these limits are very similar to the sensitivity obtained in the tabletop gravity measurement experiments.

While the data agree well with the SM predictions, the two highest-mass candidate events observed in the analysis are quite interesting. Their parameters are listed in Table VI and their displays are shown in Fig. 6. One of them is an  $e^+e^-$  event, while the other one is diphoton. Both have anomalously low value of  $|\cos \theta^*|$ , which make them typical of the topologies expected from the signal. Nevertheless, so far there is no evidence for any excess above the SM predictions. More data would show whether there is any significance in observing such low  $|\cos \theta^*|$  for the highest-mass candidate events.

Run	Event	$\cancel{E}_T$	Type	$E_T^1 (p_T^1)$	$E_T^2 (p_T^2)$	$\eta_1$	$\eta_2$	$\phi_1$	$\phi_2$	$M$	$\cos \theta^*$	$N_{\text{jet}}$
177851	28783974	8.8	$e^+e^-$	239.2 (190.8)	226.9 (234.4)	-0.45	-0.50	0.48	3.68	475	0.01	1
175826	15382214	17.0	$\gamma\gamma$	197.9	158.4	-0.47	0.87	3.20	0.06	436	0.03	0

Table VI: Parameters of the two DØ highest diEM mass candidates. Both events have only one reconstructed vertex, in a good agreement with the vertex from EM pointing. All energy variables are in GeV.

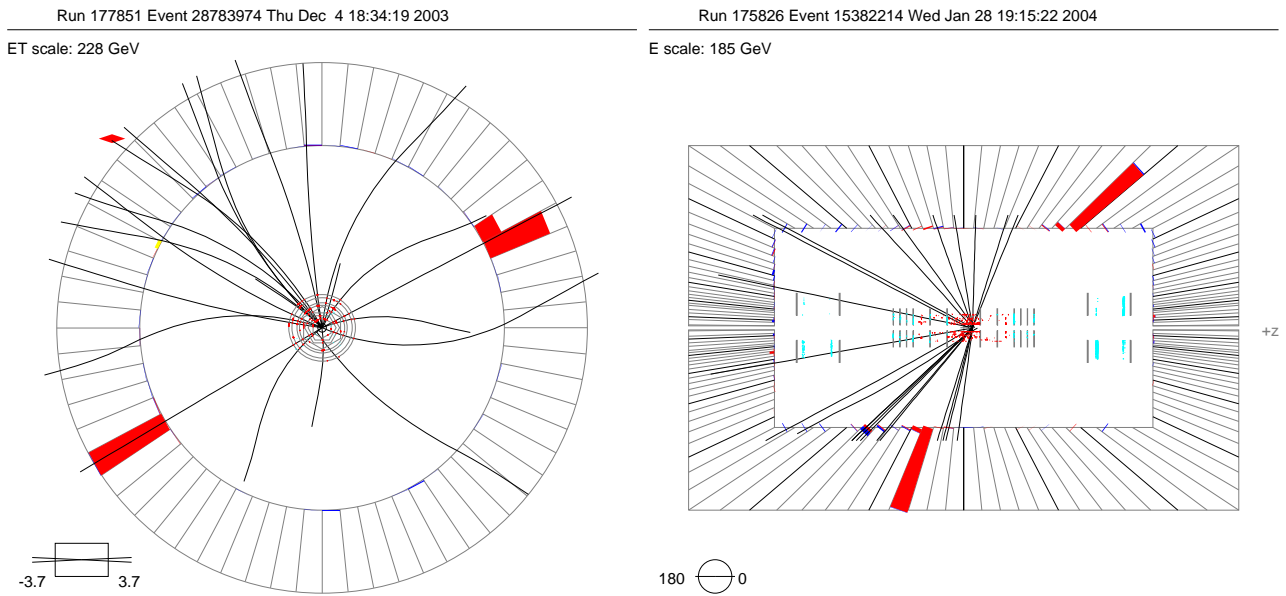


Figure 6: Left pane: event display of the highest-mass DØ  $e^+e^-$  candidate with the invariant mass of 475 GeV and  $\cos \theta^*$  of 0.01 (Run 177851, Event 28783974, or “Event Callas”). Right pane: event display of the highest-mass DØ  $\gamma\gamma$  candidate with the invariant mass of 436 GeV and  $\cos \theta^*$  of 0.03 (Run 175826, Event 15382214, or “Event Farrar”). This is the highest mass diphoton event ever observed. While in agreement with the SM background predictions, both candidates have kinematical characteristics that would be typical of a signal from large ED.

### 4.3. Search for $\text{TeV}^{-1}$ Extra Dimensions via Virtual Effects

While the sensitivity of the Tevatron to  $\text{TeV}^{-1}$ ED is expected to be inferior to that from precision measurements at LEP, much higher energy of the Tevatron make searches there complementary to those at LEP. Since there has

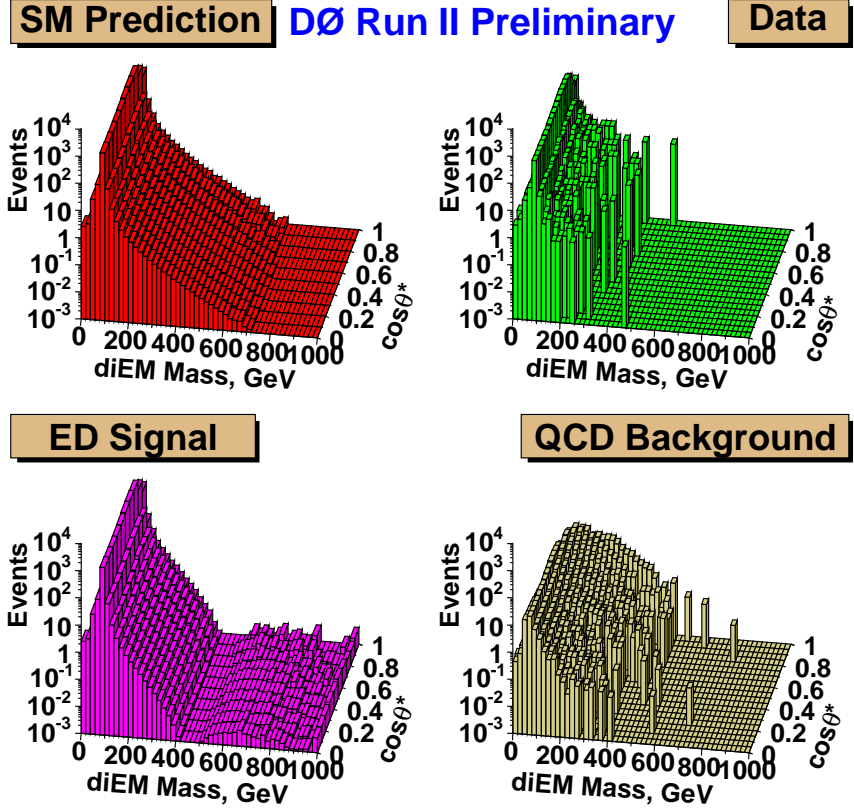


Figure 7: The  $e^+e^-$  mass vs.  $\cos\theta^*$  distribution in the DØ  $\text{TeV}^{-1}$  analysis. Top left: SM Drell-Yan background; top right: data; bottom left:  $\text{TeV}^{-1}$ ED signal plus the SM background for  $\eta_C = 5.0 \text{ TeV}^{-2}$ ; bottom right: instrumental background.

been no dedicated experimental searches for  $\text{TeV}^{-1}$  ED done at any high-energy machine, it's worth performing such a search at the Tevatron. The DØ experiment has recently obtained the first preliminary result of such a search.

The analysis follows closely that for the large ED via virtual effects, with the exception that in the case of  $\text{TeV}^{-1}$  ED, the modification of the SM cross section is due to an exchange of virtual Kaluza-Klein excitations of the SM gauge bosons. In the case of the DØ analysis, the effects of the Kaluza-Klein tower of  $\gamma$  and  $Z$  have been sought. Since  $\gamma/Z$  do not couple to photons in the SM, only the dielectron channel has been used for the analysis. The dielectrons were selected from the  $200 \text{ pb}^{-1}$  diEM sample of the large ED analysis by requiring at least one track with a good spatial match with one of the EM objects. The analysis have been performed in the same 2D-plane at the large ED analysis, as suggested in Ref. [46].

The effects of the exchange of the KK towers of the  $\gamma/Z$  can be parameterized via a bilinear function, similar to that of Eq. (6). In this case, the parameter  $\eta_G$  is replaced by  $\eta_C = \pi^2/(3M_C^2)$ , where  $M_C$  is the compactification scale,  $M_C = 1/R$ .

The data is compared with the SM background, instrumental background, and the effects from  $\text{TeV}^{-1}$  ED in Fig. 7. Again, a good agreement is observed between the data and the sum of the background predictions in the 2D-plane. The highest-mass event in the plot is the Event Callas from the large ED analysis.

Note that the effects of the  $\gamma_{\text{KK}}/Z_{\text{KK}}$  exchange are more convoluted than those for the  $G_{\text{KK}}$  exchange. Negative interference is observed at the masses approximately equal to  $M_C/2$ , which correspond to the negative interference between the DY production and the first KK modes of the  $\gamma/Z$ . Enhancement of the cross section is observed at the masses  $\sim M_C$  due to excitation of the first KK mode of  $\gamma/Z$  with low degree of virtuality.

The data is fit to the sum of the SM, interference, and direct Kaluza-Klein terms with  $\eta_C$  being a free parameter of the fit. The following 95% CL lower limit on  $M_C$  has been obtained:

$$M_C > 1.12 \text{ TeV}, \quad (7)$$

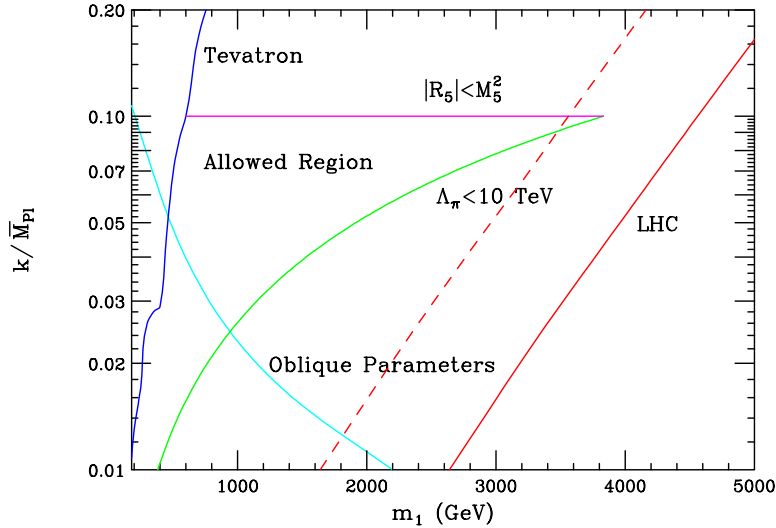


Figure 8: Allowed parameter space for parameters  $M_1$  (called  $m_1$  in the plot) and  $k/\bar{M}_{\text{Pl}}$  in the Randall-Sundrum model. The allowed region is the tooth-like shape restricted by the limits from the oblique parameters and theoretical bounds coming from the requirement of  $\Lambda_\pi < 10$  TeV and the limit on the curvature of the AdS space (horizontal line), both required in order not to create another large hierarchy of scales. Also shown in the plot are expected sensitivity of the Tevatron Run II with  $2 \text{ fb}^{-1}$  of data based on the DY channel and at the LHC with integrated luminosities of  $10 \text{ fb}^{-1}$  (dashed line) and  $100 \text{ fb}^{-1}$  (solid line marked “LHC”). From Ref. [10].

which corresponds to the limit on the size of  $\text{TeV}^{-1}$  ED  $R < 1.75 \times 10^{-19} \text{ m}$ .

#### 4.4. Searches for Randall-Sundrum Gravitons in the Dilepton and Diphoton Channels

Both the CDF and DØ collaborations performed first searches for the effects of Kaluza-Klein gravitons in the Randall-Sundrum model. As discussed above, the simplest RS model is fixed by specifying just two parameters: the curvature of the AdS space  $k$  and the radius of compactification  $R$ . However, from the experimental point of view, it is more convenient to work with an equivalent set of parameters, which correspond to the direct observables:  $M_1$ , the mass of the first Kaluza-Klein excitation of the graviton, and a dimensionless coupling  $k/\bar{M}_{\text{Pl}}$ , which governs coupling of the gravitons to the SM fields and hence the internal width of the KK gravitons. The allowed range for these two parameters is shown in Fig. ?? [10].

Both CDF and DØ collaborations used dilepton and diphoton mass spectra and searched for narrow resonances, which would indicate a production of a KK graviton. Note that even for the largest allowed value of  $k/\bar{M}_{\text{Pl}}$ , the internal width of the  $G_{\text{KK}}$  is significantly narrower than experimental mass resolution of either CDF or DØ detector, so the search has been only optimized as a function of mass. The dielectron mass spectrum used in the CDF analysis is the same as shown in Fig. 4. The dimuon and diphoton mass spectra are shown in Fig. 9 and correspond to the integrated luminosity of  $200 \text{ pb}^{-1}$  and  $345 \text{ pb}^{-1}$  respectively. All three spectra are described well by the background-only hypothesis; no narrow peaks are seen in any of the spectra.

Signal cross sections are estimated with PYTHIA [42] Monte Carlo, with the next-to-leading effects accounted for by multiplying cross sections by a constant  $K$ -factor of 1.3. At each hypothetical graviton mass a window with the size of  $\pm 3$  standard deviations due to mass resolution in the particular channel is used to count the events and the results of these counting experiments are interpreted as the limits on the RS graviton production. These limits are shown in Fig. 10 for each of the three channels. The sensitivity is dominated by the diphoton channel, not only due to the higher statistics, but also due to the fact that branching fraction of RS gravitons into diphotons is twice as large as that into a single dilepton channel. An event displays of one of the highest-mass dielectron and the highest-mass diphoton candidates from the CDF search are shown in Fig. 11.

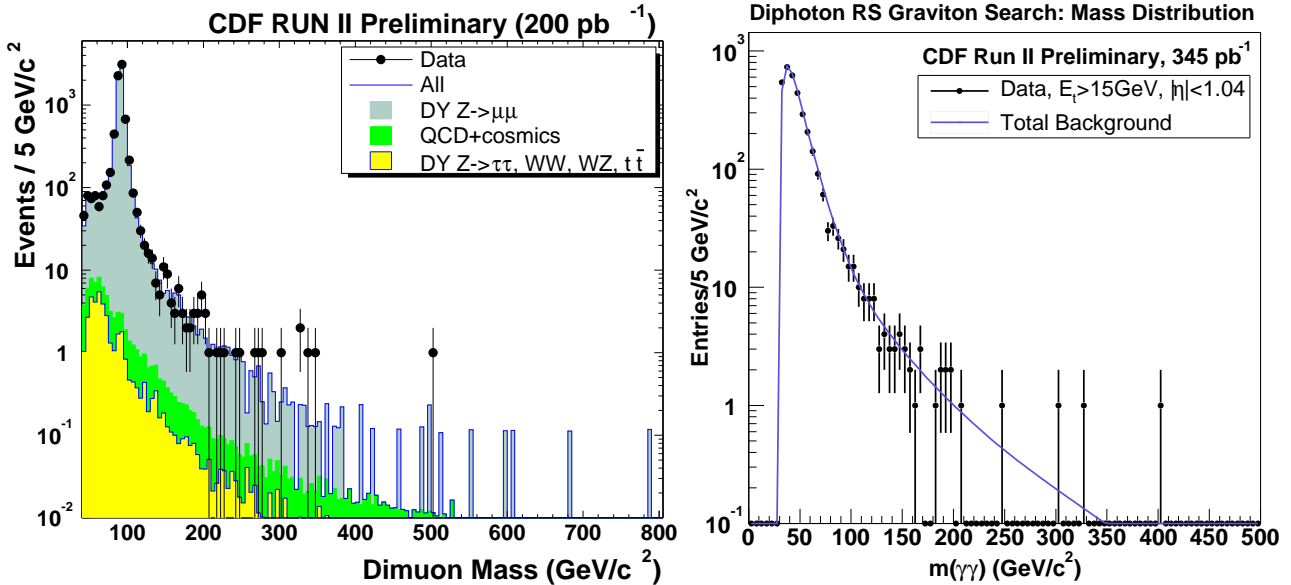


Figure 9: Dimuon (left) and diphoton (right) mass spectrum from the CDF search for Randall-Sundrum gravitons. Points are data; solid line is the total expected background.

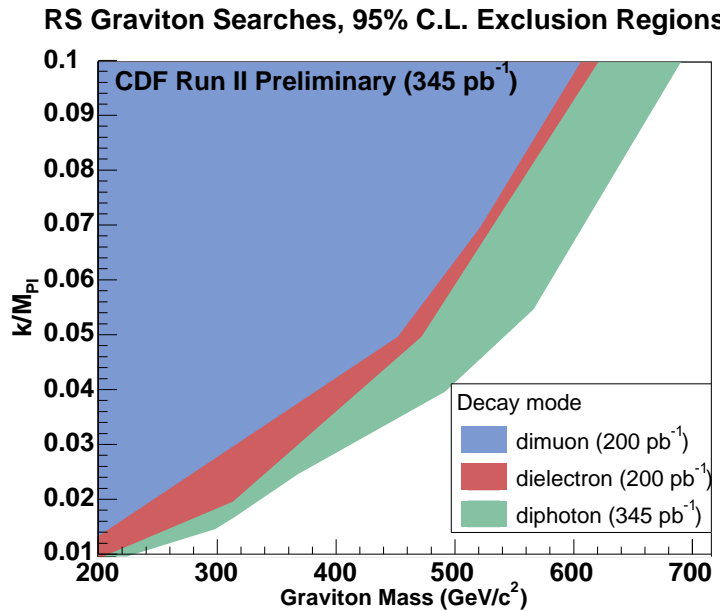


Figure 10: Individual 95% CL limits on the RS model parameters  $M_1$  and  $k/\bar{M}_{\text{Pl}}$  from the CDF search in three channels. The shaded area to the left of the corresponding curve is excluded.

The corresponding DØ search is based on the diEM candidate sample used for the search for large ED. Similar to the latter search, electrons from photons are not distinguished from one the other, which allows to combine the two channels without losing any efficiency. The analysis is based on the diEM mass spectrum shown in Fig. 12, which is simply a projection of the 2D-distribution in Fig. 5 on the mass axis. At low masses the mass window for the counting experiment was optimized to give maximum Gaussian significance ( $S/\sqrt{B}$ ) using method of Ref. [47], modified for exponentially falling background. At high masses, where background is small, the window size is chosen to be  $\pm 3$  standard deviations due to mass resolution of the DØ EM calorimeter. Signal was generated with PYTHIA [42] Monte Carlo, followed by a fast detector simulation. The event generator used in the large ED searches was used to

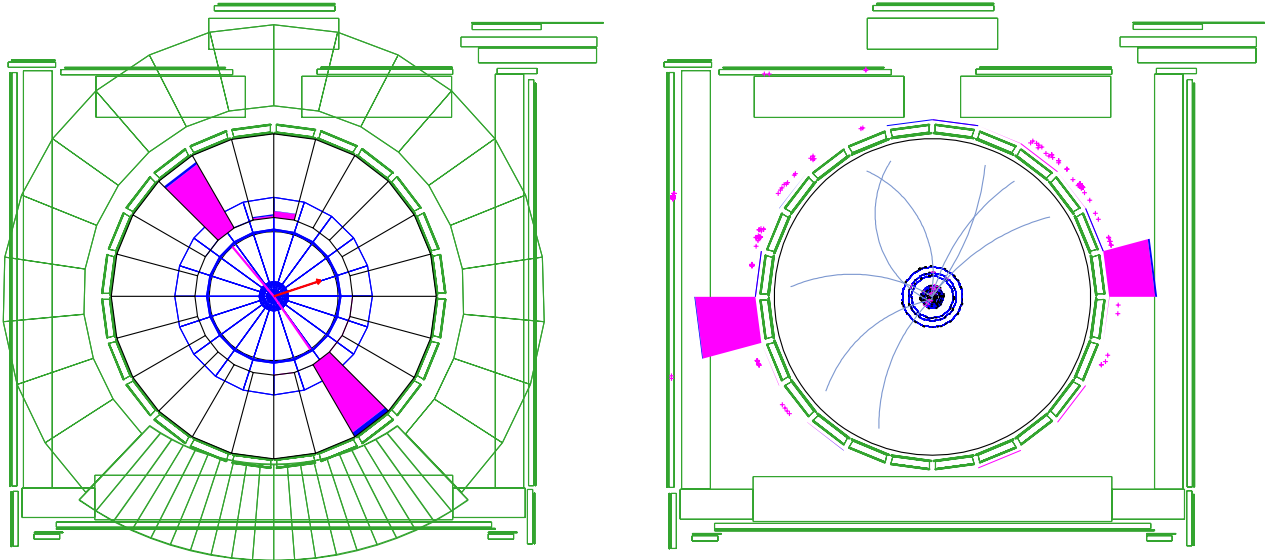


Figure 11: Left: an event display for one of the high-mass ( $M_{ee} = 371$  GeV) CDF dielectron candidate events. Right: an event display for the highest-mass ( $M_{\gamma\gamma} = 405$  GeV) CDF diphoton candidate event.

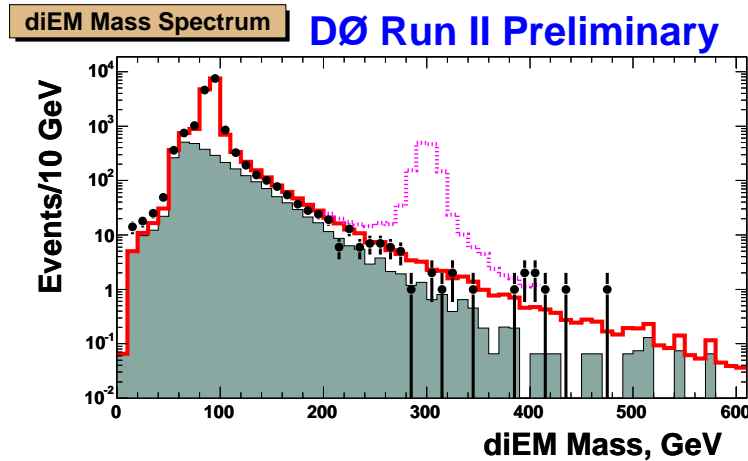


Figure 12: DiEM mass spectrum from the DØ search for Randall-Sundrum gravitons. Points are data; solid line is the total expected background; shaded histogram is the instrumental background due to jets misidentified as EM objects. Also shown in the plot a signal for a RS-graviton with the mass of 300 GeV, with arbitrary cross section normalization.

generate SM backgrounds. As in the large ED analysis, the leading order cross sections for signal and background have been multiplied by a constant  $K$ -factor of 1.3.

As in the CDF analysis, no evidence for narrow resonances is found in the DØ data, and the results are presented as limits on the RS model parameter space, shown in Fig. 13. These limits are the most stringent limits on RS model parameters to date. Note that they already exceed theoretical expectations for ten times the statistics, corresponding to the full Run II data set (see Fig. 8), due to thorough optimization and addition of the diphoton channel.

#### 4.5. Search for Extra Gauge Bosons in the Little Higgs Models

While the Little Higgs models are likely to result in a very limited phenomenology at the Tevatron energies, the first attempt to look for the additional gauge bosons expected to exist in these models has been made by the CDF Collaboration. The analysis is a straightforward extension of the search for Randall-Sundrum gravitons in the

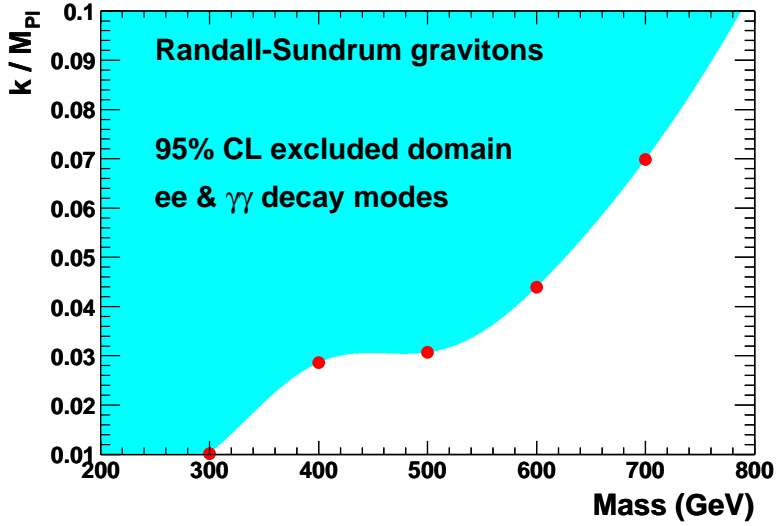


Figure 13: Combined 95% CL limits on the RS model parameters  $M_1$  and  $k/\bar{M}_{\text{Pl}}$  from the DØ search in the dielectron and diphoton channels. Dots correspond to the individual points where the counting window optimization has been done. The shaded area to the left of the curve is excluded.

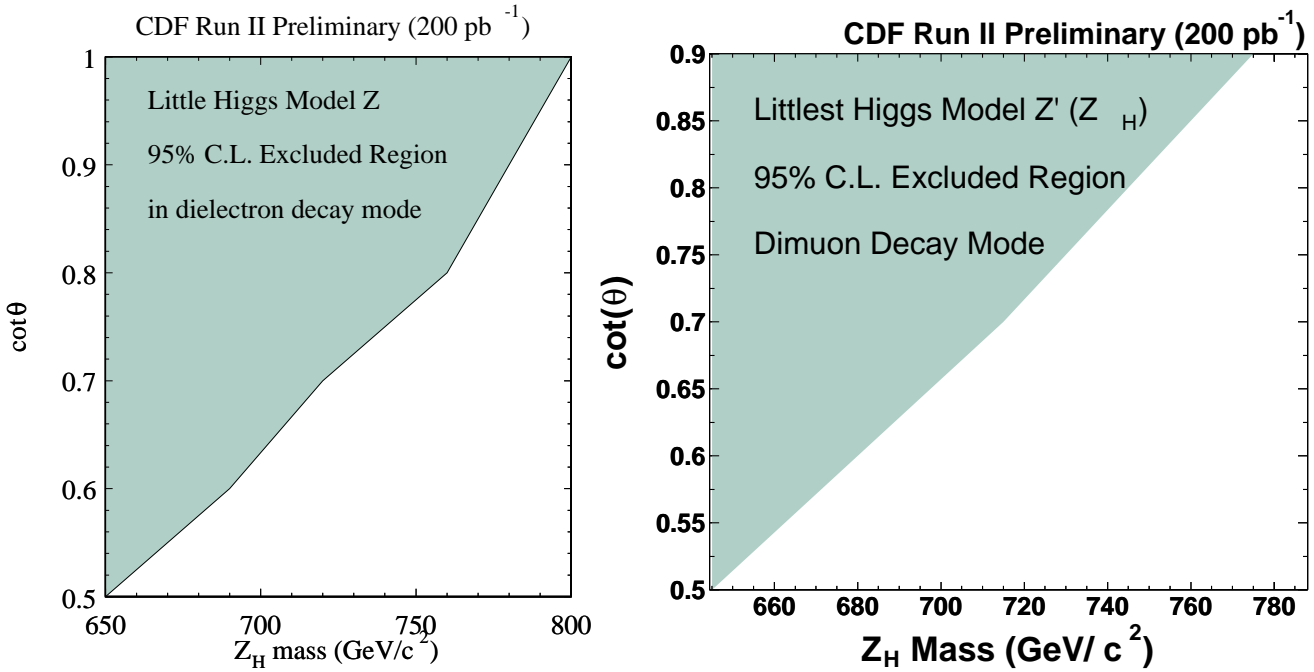


Figure 14: Individual 95% CL limits on the  $Z_H$  mass as a function of the mixing parameter  $\cot\theta$  in the little Higgs model of Ref. [17]. Left: dielectrons; right: dimuons. In each case the shaded area has been excluded.

dielectron and dimuon modes, except that the cross section limits on a hypothetical signal are interpreted as a search for a narrow  $Z_H$  resonance, which is an additional heavy  $SU(2)$  gauge boson, which is predicted in little Higgs models. The parameters that fix the couplings of the  $Z_H$  to the SM fields are discussed in Ref. [17]; the two relevant ones are the mass of the  $Z_H$  and the mixing parameter with other neutral gauge bosons,  $\cot\theta$ . Figure 14 shows the 95% CL exclusion contour obtained in this analysis. This is the first search for  $Z_H$  in the little Higgs framework at colliders.

## 5. Conclusions

Searches for low-energy effects predicted in recent models with extra spatial dimensions are one of the most exciting aspects of modern phenomenology. Various existing constraints are reviewed and the latest results from the Tevatron Run II are presented. In most of the cases they give the most stringent limits on the model parameters to date and thus opened the new level of sensitivity to the effects predicted in these various scenarios. With the Tevatron performance exceeding its design level and both the CDF and DØ experiment running smoothly and efficiently, these searches will continue at high paste and have already started probing uncharted territory in the allowed parameter space. While the LHC is the ultimate machine where new models with extra dimensions will be either confirmed or closed, the Tevatron has an exciting opportunity to either catch the first glimpse of their effects in the next few years or expand significantly the excluded parameter space. The exciting discoveries might be waiting for us just around the corner, ready to be found!

## Acknowledgments

I would like to thanks the organizers of the SSI'04 for the kind invitation and an excellent and exciting Institute. I am grateful to my colleagues in the CDF and DØ Collaborations for providing experimental results for this talk. Special thanks to Volker Buescher, Ray Culbertson, Jean-Francois Grivaz, Beate Heinemann, and Laurent Duflot. This work has been partially supported by Alfred P. Sloan Foundation, National Science Foundation under Grant #, and U.S. Department of Energy under Grant No. DE-FG02-91ER40688. Last but not the least, I am indebted to Natalie for her devotion and particularly for putting up patiently with my busy summer travel schedule.

## References

- [1] G.F.B. Riemann, “Über die Hypothesen, welche der Geometrie zu Grunde liegen,” *Abh. Ges. Wiss. Gött.* **13**, 1 (1868).
- [2] A. Einstein, *Jahrbuch der Radioaktivitaet und Elektronik* **4**, 411 (1907); A. Einstein, *Annalen der Physik* **35**, 898 (1911); *ibid.* **49**, 769 (1916); A. Einstein and M. Grossman, *Z. F. Mathematik und Physik* **62**, 225 (1913).
- [3] Th. Kaluza, *Sitzungsber. Preuss. Akad. Wiss. Phys. Math. Klasse*, 996 (1921); O. Klein, *Z. F. Physik* **37**, 895 (1926); O. Klein, *Nature* **118**, 516 (1926).
- [4] N. Arkani-Hamed, S. Dimopoulos, G. Dvali, *Phys. Lett.* **B429**, 263 (1998); I. Antoniadis, N. Arkani-Hamed, S. Dimopoulos, and G. Dvali, *Phys. Lett.* **B436**, 257 (1998); N. Arkani-Hamed, S. Dimopoulos, G. Dvali, *Phys. Rev. D* **59**, 086004 (1999); N. Arkani-Hamed, S. Dimopoulos, J. March-Russell, SLAC-PUB-7949, e-Print hep-th/9809124.
- [5] K. Dienes, E. Dudas, and T. Gherghetta, *Nucl. Phys.* **B537**, 47 (1999).
- [6] G. Giudice, R. Rattazzi, and J. Wells, *Nucl. Phys.* **B544**, 3 (1999), and revised version e-Print hep-ph/9811291.
- [7] K.R. Dienes, E. Dudas, and T. Gherghetta, *Phys. Lett. B* **436**, 55 (1998); *Nucl. Phys. B* **537**, 47 (1999); *Nucl. Phys. B* **567**, 111 (2000).
- [8] I. Antoniadis, K. Benakli, and M. Quiros, *Phys. Lett. B* **460**, 176 (1999).
- [9] L. Randall and R. Sundrum, *Phys. Rev. Lett.* **83**, 3370 (1999); L. Randall and R. Sundrum, *Phys. Rev. Lett.* **83**, 4690 (1999).
- [10] H. Davoudiasl, J.L. Hewett, and T.G. Rizzo, *Phys. Rev. Lett.* **84**, 2080 (2000); *Phys. Rev. D* **63**, 075004 (2001).
- [11] W.D. Goldberger and M.B. Wise, *Phys. Rev. Lett.* **83**, 4922 (1999).
- [12] See, e.g., K. Cheung, *Phys. Rev. D* **63**, 056007 (2001) and references therein.
- [13] T. Appelquist, H.C. Cheng, and B.A. Dobrescu, *Phys. Rev. D* **64**, 035002 (2001).
- [14] H.C. Cheng, J. Feng, and K.T. Matchev, *Phys. Rev. Lett.* **89**, 211301 (2002).
- [15] H.C. Cheng, K.T. Matchev, and M. Schmaltz, *Phys. Rev. D* **66**, 056006 (2002).

- [16] N. Arkani-Hamed, A.G. Cohen, and H. Georgi, Phys. Lett. B **513**, 232 (1991).
- [17] N. Arkani-Hamed, A.G. Cohen, E. Katz, and A.E. Nelson, JHEP **0207**, 034 (2002); N. Arkani-Hamed, A.G. Cohen, T. Gregoire, and J.G. Wacker, JHEP **0208**, 020 (2002); N. Arkani-Hamed *et al.*, JHEP **0208**, 021 (2002); for low-energy phenomenology, see, e.g. T. Han, H.E. Logan, B. McElrath, and L.T. Wang, Phys. Rev. D **67**, 095004 (2003).
- [18] C.D. Hoyle *et al.* (Eöt-Wash Collaboration), Phys. Rev. Lett. **86**, 1418 (2001); Phys. Rev. D **70**, 042004 (2004); E.G. Adelberger, e-Print hep-ex/0202008;
- [19] S. Smullin, in Proc. Intern. Summer SLAC Institute SSI'04, Stanford, 2004; URL: [http://www-conf.slac.stanford.edu/ssi/2004/lec\\_notes/Smullin/default.htm](http://www-conf.slac.stanford.edu/ssi/2004/lec_notes/Smullin/default.htm).
- [20] J. Long and J. Price, Comptes Rendus Physique **4**, 337 (2003).
- [21] S. Cullen and M. Perelstein, Phys. Rev. Lett. **83**, 268 (1999); V.D. Barger, T. Han, C. Kao, and R.J. Zhang, Phys. Lett. B **461**, 34 (1999); C. Hanhart, J.A. Pons, D.R. Phillips, and S. Reddy, Phys. Lett. B **509**, 1 (2001); C. Hanhart, D.R. Phillips, S. Reddy, and M.J. Savage, Nucl. Phys. B **595**, 335 (2001);
- [22] L. Hall and D. Smith, Phys. Rev. D **60**, 085008 (1999);
- [23] S. Hannestad and G.G. Raffelt, Phys. Rev. Lett. **88**, 071301 (2002); Phys. Rev. D **67**, 125008 (2003); M. Casse, J. Paul, G. Bertone, and G. Sigl, Phys. Rev. Lett. **92**, 111102 (2004).
- [24] M. Fairbairn, Phys. Lett. B **508**, 335 (2001); M. Fairbairn and L.M. Griffiths, JHEP **0202**, 024 (2002).
- [25] J.L. Hewett and M. Spiropulu, Ann. Rev. Nucl. Part. Sci. **52**, 397 (2002).
- [26] F. Abe *et al.* (CDF Collaboration), Phys. Rev. Lett. **74**, 2626 (1995); S. Abachi *et al.* (DØ Collaboration), Phys. Rev. Lett. **74**, 2632 (1995).
- [27] A. Gupta, N. Mondal, and S. Raychaudhuri, e-Print hep-ph/9904234.
- [28] E.A. Mirabelli, M. Perelstein, and M.E. Peskin, Phys. Rev. Lett. **82**, 2236 (1999).
- [29] J. Hewett, Phys. Rev. Lett. **82**, 4765 (1999).
- [30] T. Han, J. Lykken, and R. Zhang, Phys. Rev. D **59**, 105006 (1999), and revised version e-Print hep-ph/9811350.
- [31] S. Dimopoulos and G. Landsberg, Phys. Rev. Lett. **87**, 161602 (2001); S.B. Giddings and S. Thomas, Phys. Rev. D **65**, 056010 (2002); see also P.C. Argyres, S. Dimopoulos, and J. March-Russell, Phys. Lett. **B441**, 96 (1998); T. Banks and W. Fischler, JHEP **9906**, 014 (1999).
- [32] J.L. Feng and A.D. Shapere, Phys. Rev. Lett. **88**, 021303 (2002); see also L. Anchordoqui and H. Goldberg, Phys. Rev. D **65**, 047502 (2002); R. Emparan, M. Masip, and R. Rattazzi, Phys. Rev. D **65**, 064023 (2002); J. Alvarez-Muniz *et al.*, Phys. Rev. D **65**, 124015 (2002); L.A. Anchordoqui *et al.*, Phys. Rev. D **65**, 124027 (2002); A. Ringwald and H. Tu, Phys. Lett. B **525**, 135 (2002); S.I. Dutta, M.H. Reno, and I. Sarcevic, Phys. Rev. D **66**, 033002 (2002); Y. Uehara, Prog. Theor. Phys. **107**, 621 (2002); M. Kowalski, A. Ringwald, and H. Tu, Phys. Lett. B **529**, 1 (2002).
- [33] See, e.g., G. Landsberg, in Proc. Intern. Conference SUSY 2002, Hamburg, (2002), e-Print hep-ph/021104; M. Cavaglia, Int. J. Mod. Phys. A **18**, 1843 (2003).
- [34] LEP Exotica Working Group, ALEPH, DELPHI, L3, and OPAL Collaborations, CERN Note LEP Exotica WG 2004-03, URL: [http://lepexotica.web.cern.ch/LEPEXOTICA/notes/2004-03/ed\\_note\\_final.ps.gz](http://lepexotica.web.cern.ch/LEPEXOTICA/notes/2004-03/ed_note_final.ps.gz) and references therein.
- [35] D. Bourilkov, in Proc. 15th Les Rencontres de Physique de la Vallee d'Aoste: Results and Perspective in Particle Physics, La Thuile, Valle d'Aosta, Italy, March 2001 (2001); e-Print hep-ex/0103039.
- [36] B. Abbott *et al.* (DØ Collaboration), Phys. Rev. Lett. **86**, 1156 (2001).
- [37] V. Abazov *et al.* (DØ Collaboration), Phys. Rev. Lett. **90**, 251802 (2003).
- [38] T. Affolder *et al.* (CDF Collaboration), Phys. Rev. Lett. **89**, 281801 (2002).
- [39] T. Affolder *et al.* (CDF Collaboration), Phys. Rev. Lett. **92**, 121802 (2004).
- [40] C. Adloff *et al.* (H1 Collaboration), Phys. Lett. B **568**, 35 (2003); S. Chekanov *et al.* (ZEUS Collaboration), Phys. Lett. B **591**, 23 (2004).
- [41] K. Cheung and G. Landsberg, Phys. Rev. D **65**, 076003 (2002).
- [42] T. Sjöstrand, P. Eden, C. Friberg, L. Lönnblad, G. Miu, S. Mrenna, and E. Norrbin, Computer Physics Commun.

**135**, 238 (2001).

- [43] J. Lykken and K.T. Matchev, private communication.
- [44] U. Baur, private communication.
- [45] P. Mathews, V. Ravindran, K. Sridhar, and W.L. van Neerven, e-Print hep-ph/0411018.
- [46] K. Cheung and G. Landsberg, Phys. Rev. D **62**, 076003 (2000).
- [47] G. Landsberg and K.T. Matchev, Phys. Rev. D **62**, 035004 (2000).